

Cite this: *Analyst*, 2011, **136**, 4830

www.rsc.org/analyst

PAPER

In-line prediction of drug release profiles for pH-sensitive coated pellets

Alexey L. Pomerantsev,^{*ab} Oxana Ye. Rodionova,^a Michael Melichar,^c Anthony J. Wigmore^c
and Andrey Bogomolov^d

Received 22nd December 2010, Accepted 9th August 2011

DOI: 10.1039/c0an01033b

A new method for the prediction of the drug release profiles during a running pellet coating process from in-line near infrared (NIR) measurements has been developed. The NIR spectra were acquired during a manufacturing process through an immersion probe. These spectra reflect the coating thickness that is inherently connected with the drug release. Pellets sampled at nine process time points from thirteen designed laboratory-scale coating batches were subjected to the dissolution testing. In the case of the pH-sensitive Acryl-EZE coating the drug release kinetics for the acidic medium has a sigmoid form with a pronounced induction period that tends to grow along with the coating thickness. In this work the autocatalytic model adopted from the chemical kinetics has been successfully applied to describe the drug release. A generalized interpretation of the kinetic constants in terms of the process and product parameters has been suggested. A combination of the kinetic model with the multivariate Partial Least Squares (PLS) regression enabled prediction of the release profiles from the process NIR data. The method can be used to monitor the final pellet quality in the course of a coating process.

Introduction

Coated pellets can be used when a delayed or sustained drug release in a patient's digestive tract is necessary. The profile of an active pharmaceutical ingredient (API) release is therefore the most important criterion of the final product quality. The coating material, its thickness and coating process conditions determine the drug release kinetics.

Growth in quality standards is a pronounced trend in today's pharmaceutical production. The necessity to assure the intended product quality during a manufacturing process encourages the implementation of spectroscopic, in particular, NIR sensors for in-/on-line measurements.¹ These measurements can be conducted without process interruption or sample isolation, and therefore instantly reflect the current process state. The main principles of this approach are formulated by the U.S. Food and Drug Administration (FDA) in its Process Analytical Technology (PAT) initiative.² Monitoring the final product quality in the course of the production is one of the most challenging tasks of process analysis today.³

Spectroscopic methods, such as NIR, infrared (IR), and Raman spectroscopy are widely used for improved

understanding and monitoring of pharmaceutical processes.^{4–7} NIR spectroscopy is a well-suited technique for in-line coating monitoring.^{8–12} In particular, our previous study of the coating process has proven the feasibility of the layer thickness estimation from the in-line NIR spectra.¹³ Acquired in-line spectra cannot be used directly, as relevant information contained in the data is hidden by multiple interferences. Multivariate data analysis, a.k.a. chemometrics, is a straightforward tool to extract information from the spectroscopic data.¹⁴ Various pharmaceutical applications of NIR measurements together with the chemometric data analysis have been reported.^{8,9,15–17}

Prediction of the drug release profiles in the course of manufacturing is a challenging analytical task, which is tightly connected with the thickness and quality of the coating material.¹⁸ At present, the dissolution test is the key method for evaluating oral dosage form release. However, standard dissolution tests¹⁹ are time and labor consuming. A number of studies were devoted to the prediction of the dissolution behavior of API release using NIR spectroscopy and multivariate calibration models.^{6,12,20,21} At the same time, in all these studies analysts were aiming at establishing the direct dependence between NIR spectra and specific point in dissolution curve, *e.g.* the percentage of the released API measured at different time intervals (30 min, 1 h, *etc.*), or by correlation with the drug release percentage at a specific level, say 50%, 75%, *etc.* All these studies used the laboratory NIR data acquisition.

Our goal is to establish a procedure, which provides prediction of the drug release profile in the whole range, from 0% to 100% of the API release, using the in-line NIR measurements obtained in the course of the coating process. The study is closely related to

^aSemenov Institute of Chemical Physics RAS, Kosygin str. 4, 119991 Moscow, Russia. E-mail: forecast@chph.ras.ru; Fax: +7 495 9397483

^bState South Research & Testing Site RAS, Teatral'naya 8a, 354000 Sochi, Russia

^cGEA Pharma Systems AG, Hauptstraße 145, 4416 Bubendorf, Switzerland

^dJ&M Analytik AG, Willy-Messerschmitt-Straße 8, 73457 Essingen, Germany

the drug release mechanism. A number of previous studies have been devoted to the drug release modeling and to the analysis of the physical/chemical changes taking place during dissolution of the film-coated solid dosage forms. The term “release” encompasses several processes that contribute to the drug transfer from a dose to the bathing solution. Many researchers tend to use a so-called “hard” modeling of the drug release that relies on the physical nature of the phenomena, such as diffusion, dissolution and swelling.^{22–27} This straightforward approach may result in very accurate and predictive models. Its main disadvantage is the high mathematical complexity that in most cases leads to the absence of the explicit analytical solution. Moreover, an exhaustive understanding of the process nature is a necessary prerequisite of the hard modeling in general. In contrast to it, the “soft” models (the terminology is introduced in ref. 28) are (semi-) empirical, or data-driven. The latter strategy has also been successfully applied in dissolution studies.^{22,26,29}

The pH-sensitive polymer coatings are designed for delayed drug release. Due to the formation of an insoluble form in the acid environment, it protects the API as it travels through the stomach and then dissolves in the small intestine as the pH rises. A vast majority of the release mechanism studies of the pH-sensitive coatings deal with the final basic phase, when the dose disintegration occurs. Premature drug release in acidic media, which may happen in the case of insufficient coating thickness, is poorly studied.^{30,31} However, for the purpose of the real-time monitoring of the coating protective properties, this premature release from the undercoated process pellets is of primary interest.

The study consists of two closely related parts. Firstly, the drug release data have been modeled and a common kinetic equation, that adequately describes the profiles in a wide range of coating thicknesses and process conditions, was obtained. Secondly, the results of kinetic modeling, namely the estimates of a kinetic constant, were used as a response in PLS modeling. The predictors are NIR spectra measured in-line by means of an immersion probe in the course of the coating process. Therefore, kinetic modeling of dissolution can be viewed as data pre-processing, which extracts new variables tightly connected with the spectral data.

It is also suggested that the autocatalysis equation applied for drug release profile fitting can be considered not only as a formal but also as a physicochemical model. We think this result to be extremely important as this provides us with new information regarding the process and gives the possibility to control the process.

Material and methods

Fluid bed pellet coating

The coating material used in this study is Acryl-EZE® (Colorcon AG, Germany), the enteric formulation on the basis of a copolymer of methacrylic acid and ethyl acrylate. Two different formulations of Acryl-EZE were used; we designated them as *White* and *Yellow* grades. The difference in the coatings is that the *Yellow* one contains the addition of iron and titanium oxides. The final coat thickness applied was approximately 16 μm. This target thickness was chosen to provide the drug release times suitable for the kinetic study in the acidic medium.

The pellet coating was performed in a laboratory-scale MPI Precision Coater™ by GEA Aeromatic-Fieldler AG (Switzerland) by spraying an aqueous Acryl-EZE suspension into a concurrent fluidization of pellets, preliminarily coated with an API. The inlet air temperature was maintained at a fixed value during the batch and the coating suspension spray rate was ramped to a desired value and then held. When all the coating had been applied, the pellets were dried to the moisture content of approximately 2%. A number of the process parameters were passively monitored in real time, including temperature, pressure, and relative humidity.

Thirteen coating batches were carried out at different inlet air temperatures and spray rates spanning the possible variability of process conditions (Table 1). All batches started with 2.5 kg of nonpareil sugar/starch pellet cores (sieve size between 710 and 850 μm) by Werner's® Fine Dragées (Germany) coated with acetaminophen by Hänseler AG (Switzerland). The API-coated pellets used in this study were from a single production-scale batch to provide the homogeneity of raw material. The total sprayed mass (SM) of solid coating applied in all batches was 380 g. The coating suspension contained 15% of Acryl-EZE except for batches W1 (10%), and W2 (12.5%).

Process samples (10–20 g) for the reference analysis and the dissolution tests were taken directly from the pellet flow through a built-in “thief sampler”, located at approximately the same height as the optical probe. Nine test samples were taken from each batch at the process time points that corresponded to 12.5%, 25%, ..., 100% of the total sprayed mass. The last, ninth sampling, was performed at the end of the drying stage. In total 117 samples were collected.

In-line NIR spectra acquisition

The Lighthouse Probe™ (GEA Pharma Systems nv - Collette™, Belgium) is an immersion probe enabling in-line acquisition of diffuse-reflectance NIR spectra within a process.¹³ A J&M TIDAS 1121 SSG Spectrometer (J&M Analytik AG, Germany) with a 256-pixel diode-array detector, operating in the range from 1100 nm to 2100 nm, was used to collect spectra. SynTQ

Table 1 Batch description

Batch ID	Grade	SR ^a , g min ⁻¹	SC ^b (%)	CD ^c , min	PT ^d , min	AT ^e , °C
W1	white	24.6	10	152	170	65.7
W2	white	24.8	12.5	123	141	65.7
W3	white	26.6	15	96	113	65.8
W4	white	20	15	124	136	65.8
W5	white	28.9	15	88	104	70.8
W6	white	10.6	15	240	255	40.9
W7	white	20.5	15	124	139	58.7
Y1	yellow	16.4	15	155	167	50.8
Y2	yellow	23.6	15	108	120	60.8
Y3	yellow	14.2	15	179	190	50.7
Y4	yellow	12.9	15	198	208	53.9
Y5	yellow	26	15	98	109	72.9
Y6	yellow	20	15	127	139	59.0

^a Average spray rate during the coating phase. ^b Solid coating contents.

^c Coating phase duration. ^d Total process time (coating and drying).

^e Inlet air temperature.

software (Optimal Ltd., UK) with embedded J&M adaptor was used with the NIR-LHP for spectrometer control and data acquisition.

The time interval between the subsequent spectra was 1 min at the integration time of 75 ms. Fig. 1 illustrates the typical spectral changes during a coating process for batch W5 data. The process spectra are similar. The main difference is related to the water combination band at 1930 nm and reflects variations in the pellet moisture content. Nevertheless, minor spectral differences due to the compositional changes of pellets during the coating are sufficient to track the process in-line.¹³

Drug release study

Dissolution tests were carried out to study the kinetics of API release from the pellets in accordance with the USP paddle method.³² The following dissolution testers were used: Optimal DT-1 (Pharma Alliance Group, Inc., USA), Distek Dissolution System (Distek, Inc., USA), VanKel VK 6010, VK 3000 and VK 650 (Varian, Inc., USA). Dissolution media was 900 ml 0.1 N HCl, which corresponds to the pH value of about 1.1, with added 0.1% v/v of surfactant Tween 80 at 37 ± 0.5 °C. The paddle speed was set to 50 rpm and increased for 20 min to 250 rpm for the end samples. The samples of 5 ml for the API analysis were taken at: 15 min, 30 min, 45 min, 1 h, 1.5 h, 2 h, 3 h, 4 h, 6 h without fluid replacement. Samples passed through the 0.45 μm membrane filter before the high-performance liquid chromatographic (HPLC) analysis. HPLC (LC2010A and LC2010C, Shimadzu Corp., Japan) was conducted at 40 °C at a flow rate of 0.75 ml min^{-1} . The mobile phase was a 1 : 1 methanol/water mixture and the sample volume was 20 μL . The spectrophotometric detection was conducted at 243 nm.

The uncertainty in determination of the percentage of API release was calculated using replicated measurements, where present. Among all *White* batches the lowest standard error was 4.8% (absolute units, the percentage of the released drug) in batch W2 and the highest was 13.4% in batch W5. Unfortunately, no replicate measurements were conducted in dissolution tests for the *Yellow* batches. However, as tests were performed at the same certified laboratory using the same equipment as for *White* batches, we have to rely on the uncertainty level obtained in other tests.

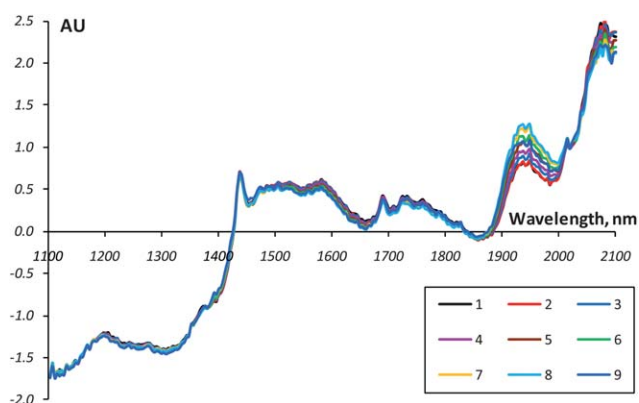


Fig. 1 NIR spectra (SNV-corrected) corresponding to the time points when sampling for the dissolution tests were performed. Batch W5.

Mathematical methods

Nonlinear regression analysis,³³ in particular, the method of successive Bayesian estimation (SBE)^{34,35} was applied for processing the dissolution tests results with the help of FITTER software.³⁶ Partial least squares (PLS)³⁷ regression modeling relating kinetic parameters to NIR spectra was performed with Chemometrics Add-In³⁸ software.

Results and discussion

Outline

This section starts with the kinetic modeling of the drug release profiles. All of them, independent of the coating material, process completeness and batch conditions, were shown to follow the same autocatalytic equation with only two constants.

Two kinetic constants of individual release profiles were then thoroughly investigated. One of them was found to be associated with the coating material type, and thus, its common estimate can be calculated from the release kinetic data of the entire set of similar batches using the nonlinear regression modeling. The other constant is closely related to the applied coating thickness, and consequently, can be predicted from the process NIR spectra. The combination of nonlinear fitting of the release kinetic curves with PLS regression analysis of the spectral data enables the prediction of drug release profiles from the in-line NIR spectra. Besides, an interpretation of the autocatalytic equation in terms of the release mechanism has been suggested on the basis of the above findings.

The discussion of results is concluded by the method validation and the description of a routine procedure for the modeling and prediction of the drug release kinetics.

Release profile modeling

The nonlinear regression method (NLR) was used for the modeling of the API release curves, *i.e.* percentage of the API release D versus time. For this purpose a kinetic model $\varphi(t, \mathbf{u})$, *i.e.* a function that depends on time t and vector of unknown parameters \mathbf{u} , was selected. Parameter estimates were chosen so that an objective function

$$Q(\mathbf{u}) = S(\mathbf{u}) + B(\mathbf{u}) \quad (1)$$

is minimized. The first term in eqn (1) is the sum of squares

$$S(\mathbf{u}) = \sum_i (D_i - \varphi(t_i, \mathbf{u}))^2 \quad (2)$$

where D_i is the API release data value, and φ is the API release model. The second term in eqn (1) is the Bayesian information, which is described below (see eqn (7)).

The minimization procedure provides the parameter estimate $\hat{\mathbf{u}}$ and the residual sum of squares $Q_0 = Q(\hat{\mathbf{u}})$. This further yields the residual variance s^2 , and the residual standard deviation (RSD) s calculated by eqn (3)

$$s^2 = \frac{Q_0}{N-p}; \quad s = \sqrt{s^2} \quad (3)$$

Here $N-p$ is the number of degrees of freedom (DoF), N is the number of samples and p is the number of unknown parameters.

It has been found that the following model

$$\varphi(t, m, k) = 100k \frac{\exp[(m+k)t] - 1}{m + k \exp[(m+k)t]} \quad (4)$$

adequately describes the API release kinetics for all pellet samples. Here t stands for time, m and k are unknown parameters, *i.e.* $\mathbf{u} = (m, k)$.

Eqn (4) is a well-known autocatalytic model that corresponds to the following reaction scheme:



where φ is a percent concentration of B, and concentrations of A and B are constrained by the following conditions $\%A + \%B = 100\%$ with initial value $\%B_0 = 0\%$. The parameters $m = 100r_1$ and $k = r_2$ have the inverse time (min^{-1}) units. Autocatalysis is a phenomenon when a process is catalyzed by its own product.³⁹ Two kinetic constants correspond to two stages: the second-order reaction catalyzed by product B (r_1), and the first order generation of B (r_2). The product accumulation leads to acceleration, which accounts for the sigmoid shape of the concentration profiles. Generally, the parameter m is responsible for the profile growth rate (slope), while k reflects the length of the induction period (delay).

Experimental justification of this mechanism is still important but this is beyond the scope of this study. Nevertheless, it can be shown that the suggested model has a solid physical background. When applied to the modeling of a large number of release profiles the model (eqn (4)) reveals interesting regularities that could not appear in the case of a purely empirical fitting. A key feature of the suggested model is the possibility to fit each release profile in the whole studied range of the process conditions with only two parameters.

The data under consideration comprise 13 batches, which are numbered by index b . Each batch consists of 9 dissolution profiles, which are numbered by index j . Each dissolution profile consists of 9 time-consecutive measurements, numbered by index i . For example, the data associated with each batch could be described as a 9×9 matrix \mathbf{D} where D_{ij} corresponds to the i -th time measurement associated with the j -th dissolution profile. Such a hierarchical data arrangement challenges a multistep data processing.

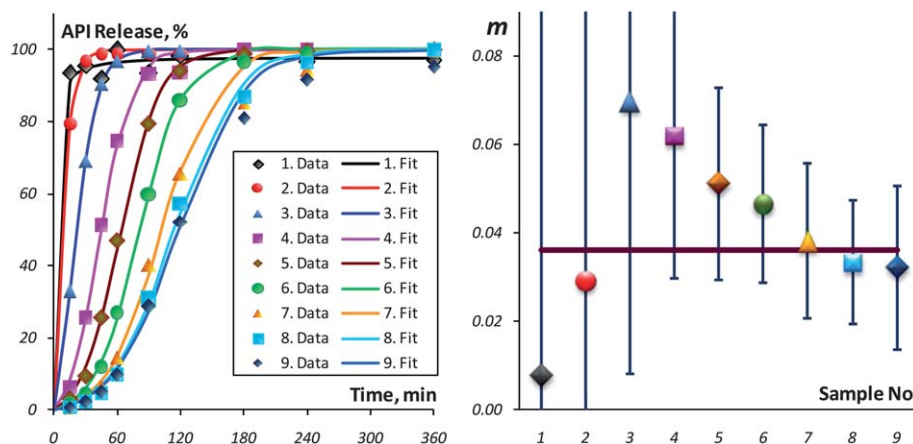


Fig. 2 Experimental data and fitting results for batch Y6. Left panel: percentage of API release vs. time; experimental data are markers, fitting curves are solid lines. Right panel: estimates for parameter m ; values \hat{m}_{bj} ($j = 1, \dots, 9$) with the 99% confidence intervals.

On the first step all dissolution profiles are fitted independently. Minimizing $13 \times 9 = 117$ objective functions given in eqn (5)

$$Q_{bj}(m, k) = \sum_i (D_i - \varphi(t_i, m, k))^2 \quad (5)$$

one can find $13 \times 9 = 117$ values \hat{m}_{bj} , \hat{k}_{bj} that estimate the parameters m and k .

Fig. 2 (left panel) shows the fitting results of batch Y6 with the autocatalytic model eqn (4). Estimates and the 99% confidence intervals for parameter m , calculated separately for each process time point (sample), are presented in Fig. 2 (right panel). Comparing these values one can conclude that the m value is common for all profiles within a batch.

Using this consideration, on the second step we minimized 13 objective functions given in eqn (6), which correspond to 13 batches ($b = 1, \dots, 13$)

$$Q_b(m, k) = \sum_{ij} (D_{ij} - \varphi(t_{ij}, m, k))^2 \quad (6)$$

and found 13 estimates \hat{m}_b for parameter m and $13 \times 9 = 117$ estimates \hat{k}_{bj} for parameter k .

The results are presented in Fig. 3.

Analysis of all estimates of parameter m leads to further generalization. All individual batches within the same Acryl-EZE formulation can be fitted by the autocatalytic model with only two parameters: m^W that is common for the *White* subset and m^Y that is common for the *Yellow* one. For the calculation of these estimates it is necessary to minimize two objective functions Q with many unknown parameters: for the *White* batches the number of parameters is equal to $64 = 1 + 9 \times 7$, and for the *Yellow* batches the number of unknown parameters is equal to $55 = 1 + 9 \times 6$. Such NLR problems are rather complicated to be solved directly. Therefore, we have applied the successive Bayesian estimation method to calculate m^W and m^Y from the data of corresponding batches.

Successive Bayesian estimation (SBE)

The SBE idea is rather straightforward. Batches are processed not simultaneously but successively, one by one. During such

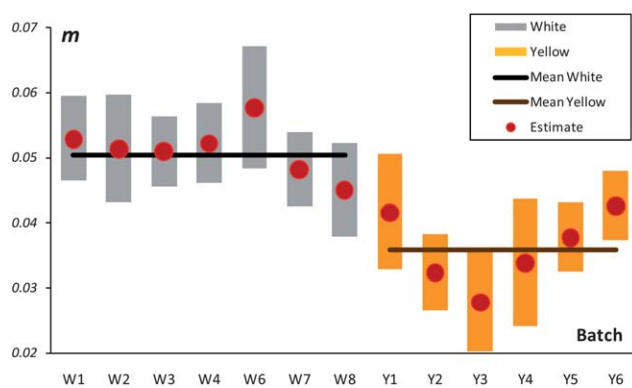


Fig. 3 Estimated values for parameters \hat{m}_b and the 99% confidence intervals.

a fitting the estimates that have been found in the previous batch are further used as *a priori* information for processing of the next batch. The SBE algorithm is as follows. Let us consider the case when the $b-1$ batches have already been processed and batch b is to be fitted. The following objective function is minimized on the b -th step

$$Q_b(m, k) = S_b(m, k) + B_b(m) = \sum_{ij} (D_{ij} - \varphi(t_{ij}, m, k))^2 + s_{b-1}^2 [N_{b-1} + H_{b-1}(m - \hat{m}_{b-1})^2] \quad (7)$$

In eqn (7) the first term, S , is the sum of squares for batch b . The second term B is *a priori* information that depends on the following values found at previous step $b-1$.

s_{b-1}^2 is the residual variance estimate;

N_{b-1} is the number of degrees of freedom;

\hat{m}_{b-1} is the estimate for parameter m ;

H_{b-1} is the information matrix (in our case it is a scalar).

The first batch ($b = 1$) is processed without *a priori* information ($H = 0$). The value of the common parameter m obtained at the last step is further used as an ultimate estimate of m . Thereupon the partial parameters k are consequently recalculated applying this m value and *a posteriori* information built after the last SBE step. Detailed description of SBE is presented in.^{33,34} Results of the final m^W and m^Y estimations are presented in Table 2.

Values in the last column of Table 2 can be compared with the measurement errors in the dissolution tests (see section Drug release study).

Simultaneously, we obtain a set of estimates \hat{k}_{bj} for the partial parameters k . The analysis of these values reveals their profound relation to the sprayed mass (SM) process macroparameter. The logarithm of k ($q = -\ln(k)$) manifests a clear linear dependence

Table 2 Results of fitting of subsets *White* and *Yellow*

Subset	Estimate \pm STD ^a	DoF ^b	RSD ^c
White m^W	0.050 \pm 0.001	1290	5.0
Yellow m^Y	0.036 \pm 0.001	394	4.8

^a Standard deviation. ^b Number of degrees of freedom. ^c Residual standard deviation.

on SM (Fig. 4) in all studied batches. This is in line with the result reported in.⁴⁰

Thus, parameter m in model eqn(4) seems to inhere in both *White* and *Yellow* subsets as reflecting the material grade. In contrast to it, k is individual for each profile with exponential dependence on the sprayed mass. As the sprayed mass is directly linked to the coating thickness, it can be concluded that parameter k essentially reflects the polymer layer growth during the coating process. At the same time, Fig. 4 (right panel) shows that the linear dependences of q against SM in different batches are not the same. This observation reflects the fact that the kinetics of API drug release depends not only on the coating thickness, but also on the coating quality. The latter, in its turn, depends on manufacturing conditions (see Table 1), such as coating temperature, spray rate, *etc.* This result shows that the PAT procedure based on model eqn (4) has a possibility to account for a batch singularity and therefore control each individual coating process in its progress.

In the left panel of Fig. 4 the 99% confidence intervals are shown. Similar intervals in the right panel are not presented for clarity of the picture. They are of similar sizes.

Analysis of NIR spectra

It has been shown that in the course of the kinetic data modeling, it is possible to estimate the value of parameter m , which characterizes the coating material. However, for the prediction of the drug release profile it is necessary to estimate the value of k , which is changing during the manufacturing process. As the pellet coating thickness and the drug release process are tightly connected, one can use the NIR data for the prediction of this parameter.

The NIR spectra closest to the sampling process time points were selected for modeling (Fig. 1). The predictor matrices \mathbf{X} comprise $7 \times 9 = 63$ NIR spectra from the *White* subset, and $6 \times 9 = 54$ NIR spectra from the *Yellow* subset. The response vectors \mathbf{y} consists of the $q_{\text{NLR}} = -\ln(k)$ values calculated by the kinetic modeling of the release profiles. Prior to modeling, the NIR spectra are pre-treated by the standard normal variate (SNV) procedure.¹⁴ SNV is known to be effective to compensate for the variable spectral baselines and intensities caused by the process dynamics.

The partial least squares (PLS)³⁷ regression method is applied for the development of the calibration models. The number of PLS latent variables (LV) is determined using values of the root mean square error (RMSE) of calibration, RMSEC, the segmented 10%-out cross-validation,³⁷ RMSECV, and explained variances for predictors and response (see Fig. 5, Fig. 6 and Table 3).

Two individual PLS regression models were built for the *White* and *Yellow* subsets. The residual analysis has shown that samples with the ordinal number 1 acquired at the beginning of the *Yellow* process are outliers. Virtual absence of the protective coating of the initial samples is a straightforward explanation of this fact. Therefore, these samples were excluded from the PLS modeling of the *Yellow* subset.

The model statistics are presented in Table 3. The good model performances are illustrated by Fig. 5 and Fig. 6. Considering that the modeling was based on the representative set of designed coating batches, a reasonable number of latent PLS variables

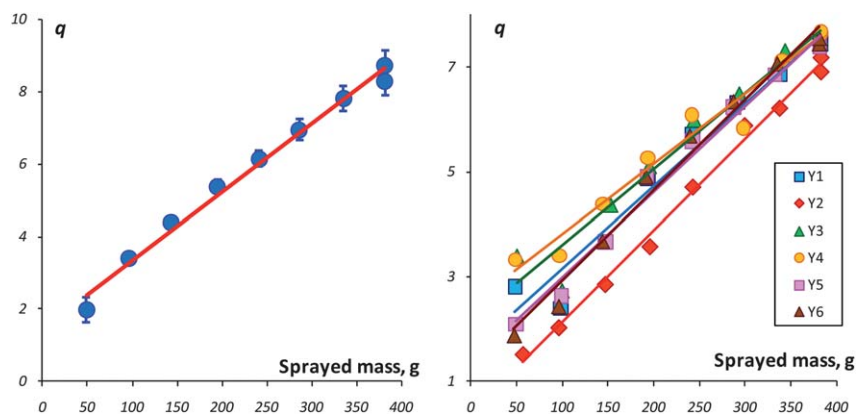


Fig. 4 Dependence of $q = -\ln(k)$ against sprayed mass: (left) Batch W1 from subset *White* 99% confidence intervals are shown; (right) All batches from subset *Yellow*.

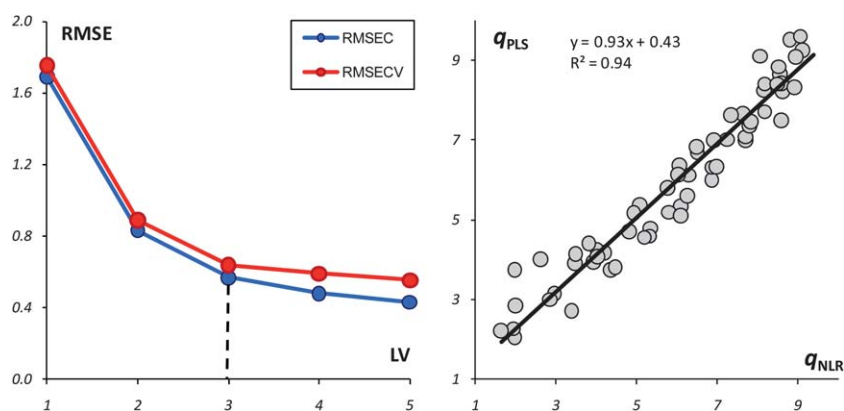


Fig. 5 PLS model for the subset *White*. Left panel: RMSEC and RMSECV vs. number of LV. Right panel: Performance in prediction of q_{PLS} predicted by cross-validation vs. q_{NLR} , used as response in PLS modeling.

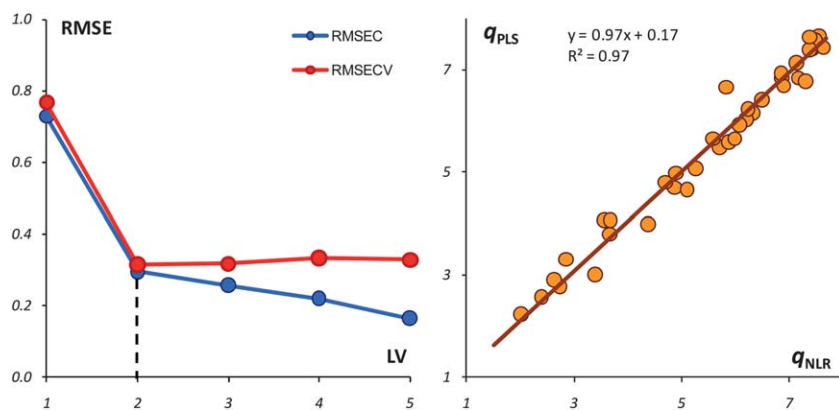


Fig. 6 PLS model for the subset *Yellow*; Left panel: RMSEC and RMSECV vs. number of LV. Right panel: Performance in prediction of q_{PLS} predicted by cross-validation vs. q_{NLR} , used as response in PLS modeling.

(LV = 3 for the *White* subset and LV = 2 for the *Yellow*) indicates a high model sustainability in the prediction of new samples.

Test set validation

To validate the prediction capability of the proposed approach, batches W2, and Y5, nine samples each, were excluded from the

calibration sets to be taken as a new data for prediction. Consequently, for the *White* subset the calibration set comprised six batches (W1, W3–W7) and for the *Yellow* subset - five batches (Y1–Y4, Y6). Estimates m^w and m^y , calculated using the reduced calibration subsets insignificantly differed from those calculated using the whole data sets. Two PLS regression models for $q = -\ln(k)$ were established with the same numbers of LVs as in

Table 3 PLS modeling and validation statistics in prediction of $q_{\text{NLR}} = -\ln(k)$ from the NIR spectra matrix, \mathbf{X}

Subset	LV	X explained	q_{NLR} explained	RMSEC	RMSECV	R^2
White	3	88.2%	92.7%	0.58	0.64	0.93
Yellow	2	95.0%	92.9%	0.24	0.28	0.97

the full models (3 and 2 for the *White* and *Yellow* subsets respectively). Then, these models were used to predict kinetic parameters k for test batches W2 and Y5. Predicted API release curves for W2 and Y5 are presented in Fig. 7 and Fig. 8 respectively.

Several data points (four in batch W2 and two in batch Y5) can be considered as outliers. They are shown with the unfilled markers.

The quality of prediction can be evaluated by comparison of the residual standard deviations (RSD) obtained at different levels of batches W2 and Y5 modeling. At the initial stage, when both batches were included in the full datasets, they have been modeled with individual “calibration” RSDs that were: $s^{\text{W}2} = 5.9$, $s^{\text{Y}5} = 3.4$. During the validation, when W2 and Y5 are in the test set, “prediction” RSDs are: $s^{\text{W}2} = 6.5$, $s^{\text{Y}5} = 4.6$. Furthermore “prediction” RSDs can be compared with the dissolution test

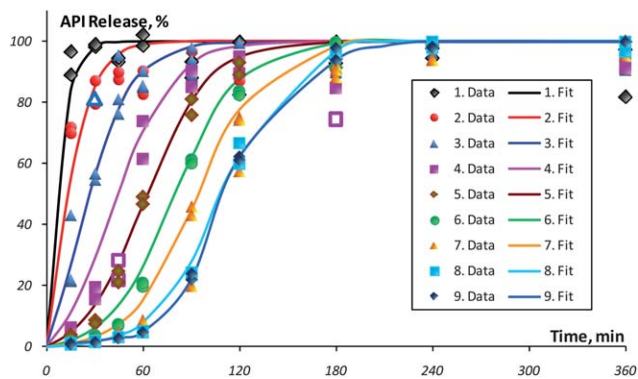


Fig. 7 Predicted API release curves for batch W2 (subset *White*); hollow markers designate outliers.

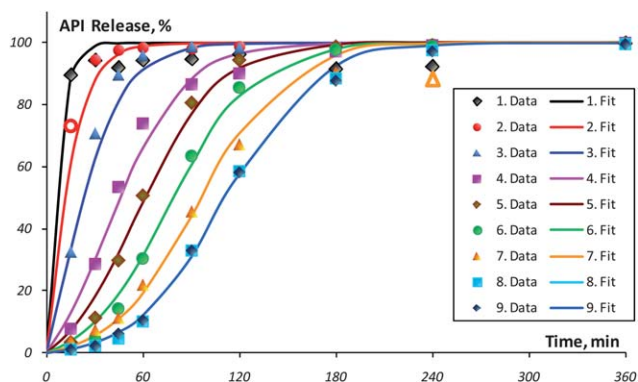


Fig. 8 Predicted API release profiles for batch Y5 (subset *Yellow*); hollow markers designate outliers.

Table 4 Modeling and prediction statistics for nine process time points (samples) in W2 and Y5

Sample	Batch W2				Batch Y5			
	q_{NLR}^a	q_{PLS}^b	RSDC ^c	RSDP ^d	q_{NLR}^a	q_{PLS}^b	RSDC ^c	RSDP ^d
1	1.94	1.79	7.67	8.32	2.09	1.79	6.03	6.35
2	2.96	2.99	8.95	9.66	2.63	2.99	1.21	5.14
3	4.20	4.13	6.67	6.70	3.67	4.13	2.85	4.65
4	5.80	5.03	7.91	8.41	4.89	5.03	4.24	4.97
5	6.28	5.69	3.72	4.51	5.58	5.69	3.39	4.00
6	7.24	6.26	3.09	4.94	6.23	6.26	2.91	3.06
7	8.14	6.95	5.93	5.50	6.85	6.95	2.92	5.07
8	8.54	7.39	2.00	3.21	7.38	7.39	2.04	2.06
9	8.61	7.65	1.52	4.88	7.38	7.65	2.17	4.25

^a NLR estimate of q . ^b PLS estimate of q . ^c Residual standard deviation in calibration. ^d Residual standard deviation in prediction.

standard error of 4.8 calculated from the replicated measurements in batch W2.

Table 4 presents the prediction statistics of the drug release kinetics in more details and a comparison with the fitting quality. As a rule, the fitting accuracy (when a batch is a member of the calibration set) is higher in comparison with the case when the batch is used as a test set. Columns q_{NLR} and **RSDC** present values calculated when batches W2 and Y5 were included in the calibration set and Columns q_{PLS} and **RSDP** present corresponding values in the case of W2 and Y5 only being used for prediction.

Routine modeling and prediction procedure

To develop a routine procedure for the release profile prediction from in-line process NIR spectra, the following steps are performed. Primarily, the dissolution tests data are processed by the SBE method. This provides the estimate for parameter m in eqn (4), and also determines a set of parameters $\mathbf{q} = \{-\ln(k_{ij})\}$, values of which are changing in the course of the coating process. After that, the PLS model, which regress \mathbf{q} on spectral data \mathbf{X} is established. As a result, the calibration model $\mathbf{q} = \mathbf{X}\mathbf{a}$ together with eqn (4), can be used in the routine analysis to yield a whole dissolution curve for each spectral measurement conducted in-line. Such a curve is obtained directly by means of a kinetic model (eqn (4)) with the known parameter m and parameter $k = \exp(-q)$, which is calculated by the PLS model as soon as the NIR spectrum is acquired. In the case that the coating material is changed, the model should be updated.

The modeling and prediction flowchart is schematically presented in Fig. 9.

Therefore, the suggested approach enables an accurate prediction of the release profiles with the uncertainty that is comparable to that of the dissolution tests (see section Drug release study). Moreover, the constraints prescribed by the kinetic model (eqn (4)) tend to “fix” the noticeable outliers in the experimental data, manifested in the seeming concentration decrease or not reaching the 100%-level after the dissolution completeness (Fig. 7 and Fig. 8).

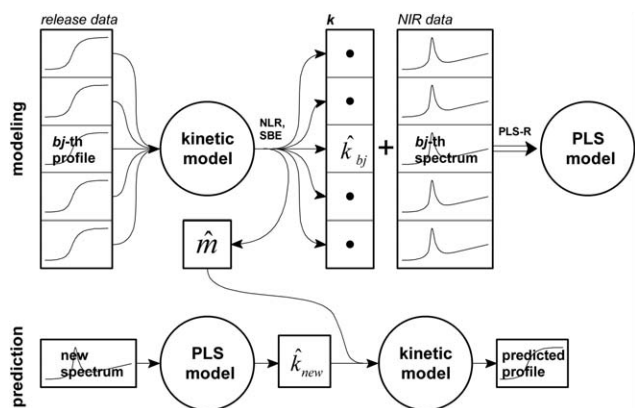


Fig. 9 Modeling and prediction flowchart.

Conclusions

Summarizing both the theoretical outcomes and practical outputs of the research, the following points should be highlighted.

A valuable theoretical result is the solution of the “curve-to-curve” calibration problem and in the particular case considered here, the prediction of the drug release profiles from NIR spectra. This method differs from the conventional approach, where a curve is restored from the individually calibrated and predicted points. The advocated approach extracts new features as the parameters of a function approximating the drug release profile. Such a function can be selected on a purely empirical basis, or derived from the fundamental process knowledge. Additionally, successful approximation results in a considerable data reduction. The main merit however is the ability to predict the whole curve smoothly.

It has been found that the autocatalytic model perfectly fits the drug release kinetics of the pellets coated by a pH-sensitive polymer. Moreover, two underlying kinetic constants have a reasonable physical interpretation. The first parameter, m , is responsible for the coating material grade and this parameter varies neither within a batch nor between the similar batches. The second parameter, k , is closely related to the coating thickness and this dependence is individual for every batch. Subsequently, the autocatalysis is a mechanical rather than a purely empirical model. A preliminary explanation of the mechanism's nature has been suggested.

Application of the kinetic model in combination with the PLS regression results in a practical PAT method for prediction of the drug release profiles from the in-line NIR spectra. In this procedure the parameter m is estimated in advance from the relevant dissolution tests. The value of m does not vary as long as the coating material is the same. The parameter k is predicted from the NIR spectra using PLS calibration. With each new spectrum obtained during the coating, the value of k changes. The main advantage of the method is that the procedure continuously accounts for the individual peculiarities of a current batch at any process time point. Thus, the combination⁴¹ of the hard (autocatalytic model) and the soft (multivariate regression) methods serves as a very efficient technique for real-time drug release analysis.

Acknowledgements

The authors thank Joachim Mannhardt for his helpful efforts during the project time. The PANOPOD-II project (AZ 25304/02) has been supported by Deutsche Bundesstiftung Umwelt (DBU).

References

- 1 J. Aaltonen, K. C. Gordon, C. J. Strachan and T. Rades, *Int. J. Pharm.*, 2008, **364**, 159–169.
- 2 <http://www.fda.gov/downloads/Drugs/GuidanceComplianceRegulatory-Information/Guidances/UCM070305.pdf> [20 December 2010].
- 3 S. Wold, J. Cheney, N. Kettaneh and C. McCready, *Chemom. Intell. Lab. Syst.*, 2006, **84**, 159–163.
- 4 J. Workman Jr., M. Koch, B. Lavine and R. Chrisman, *Anal. Chem.*, 2009, **81**, 4623–4643.
- 5 J. Rantanen, H. Wikstro, R. Turner and L. S. Taylor, *Anal. Chem.*, 2005, **77**, 556–563.
- 6 M. Blanco, M. Alcalá, J. M. Gonzales and E. Torras, *J. Pharm. Sci.*, 2006, **95**, 2137–2144.
- 7 S. Matero, S. Poutiainen, J. Leskinen, S.-P. Reinikainen, J. Ketolainen, K. Järvinen and A. Poso, *J. Chemom.*, 2008, **22**, 644–652.
- 8 Y. Roggo, P. Chalus, L. Maurer, C. Lema-Martinez, A. Edmond and N. Jent, *J. Pharm. Biomed. Anal.*, 2007, **44**, 683–700.
- 9 J. J. Moes, M. M. Ruijken, E. Gout, H. W. Frijlink and M. I. Ugwoke, *Int. J. Pharm.*, 2008, **357**, 108–118.
- 10 M. Andersson, S. Folestad, J. Gottfries, M. O. Johansson, M. Josefson and K.-G. Wahlund, *Anal. Chem.*, 2000, **72**, 2099–2108.
- 11 M. Andersson, M. Josefson, F. W. Langkilde and K.-G. Wahlund, *J. Pharm. Biomed. Anal.*, 1999, **20**, 27–37.
- 12 R. P. Cogdill, R. N. Forcht, Y. Shen, P. T. Taday, J. R. Creekmore, C. A. Anderson and J. K. Drennen III, *J. Pharm. Innovation*, 2007, **2**, 29–36.
- 13 A. Bogomolov, M. Engler, M. Melichar and A. Wigmore, *J. Chemom.*, 2010, **24**, 544–557.
- 14 T. Naes; T. Isaksson; T. Fearn; T. Davies *Multivariate Calibration and Classification*. NIR Publications: Chichester, UK, 2002.
- 15 O. Ye. Rodionova, A. L. Pomerantsev, L. Houmuller, A. V. Shpak and O. A. Shpigun, *Anal. Bioanal. Chem.*, 2010, **397**, 1927–1935.
- 16 O. Ye. Rodionova, Ya. V. Sokovikov and A. L. Pomerantsev, *Anal. Chim. Acta*, 2009, **642**, 222–227.
- 17 O. Ye. Rodionova, L. P. Houmøller, A. L. Pomerantsev, P. Geladi, J. Burger, V. L. Dorofeyev and A. P. Arzamastsev, *Anal. Chim. Acta*, 2009, **549**, 151–158.
- 18 J. D. Kirsch and J. K. Drennen, *J. Pharm. Biomed. Anal.*, 1995, **13**, 1273–1281.
- 19 V. Gray, G. Kelly, M. Xia, C. Butler, S. Thomas and S. Mayock, *Pharm. Res.*, 2009, **26**, 1289–1302.
- 20 M. P. Freitas, A. Sabadin, L. M. Silva, F. M. Giannotti, D. A. do Couto, E. Tonhi, R. S. Medeiros, G. L. Coco, V. F. T. Russo and J. A. Martins, *J. Pharm. Biomed. Anal.*, 2005, **39**, 17–21.
- 21 S. H. Tabasi, V. Moolchandani, R. Fahmy and S. H. Hoag, *Int. J. Pharm.*, 2009, **382**, 1–6.
- 22 P. Macheras; A. Iliadis, *Modeling in Biopharmaceutics, Pharmacokinetics, and Pharmacodynamics. Homogeneous and Heterogeneous Approaches*, Springer: New York, 2006.
- 23 N. A. Peppas, J. C. Wut and E. D. von Meerwall, *Macromolecules*, 1994, **27**, 5626–5638.
- 24 P. I. Lee, *Pharm. Res.*, 1993, **10**, 980–985.
- 25 G. Frenning, A. Tunón and G. Alderborn, *J. Controlled Release*, 2003, **92**, 113–123.
- 26 S. Ensslin, K. P. Moll, K. Paulus and K. Mäder, *J. Controlled Release*, 2008, **128**, 149–156.
- 27 M. Marucci, G. Ragnarsson, U. Nyman and A. Axelsson, *J. Controlled Release*, 2008, **127**, 31–40.
- 28 M. Pidd. *Tools for thinking: modelling in management science*, Wiley: 2003.
- 29 M. Grassi and G. Grassi, *Curr. Drug Delivery*, 2005, **2**, 97–116.
- 30 H. X. Guo, J. Heinämäki and J. Yliruusi, *Int. J. Pharm.*, 2002, **235**, 79–86.

-
- 31 F. Siepmann, C. Wahle, B. Leclercq, B. Carlin and J. Siepmann, *Eur. J. Pharm. Biopharm.*, 2008, **68**, 2–10.
- 32 UPS29-NF24, 2006, pp. 2676–2677, ISBN 1-889788-39-2.
- 33 E. V. Bystritskaya, A. L. Pomerantsev and O. Ye. Rodionova, *J. Chemom.*, 2000, **14**, 667–692.
- 34 G. A. Maksimova and A. L. Pomerantsev, *Industrial Laboratory*, 1995, **61**, 432–436.
- 35 A. L. Pomerantsev, *Chemom. Intell. Lab. Syst.*, 2003, **66**, 127–139.
- 36 Fitter Add-In., <http://polycert.chph.ras.ru/fitter.htm> [20 December 2010].
- 37 A. Höskuldsson. *Prediction Methods in Science and Technology*, Thor Publishing: Copenhagen, Denmark, 1996.
- 38 Chemometrics Add-In. http://rcs.chph.ras.ru/Tutorials/projection_en.htm [20 December 2010].
- 39 M. Maeder, *Practical Data Analysis in Chemistry*, Elsevier: 2007.
- 40 T. Ishibashi, H. Hatano, M. Kobayashi, M. Mizobe and H. Yoshino, *Int. J. Pharm.*, 1998, **168**, 31–40.
- 41 A. L. Pomerantsev and O. Ye. Rodionova, *Chemom. Intell. Lab. Syst.*, 2005, **79**, 73–83.